IEEE Access
Multidisciplinary ⋮ Rapid Review ⋮ Open Access Journal

Received April 2, 2020, accepted April 17, 2020, date of publication April 27, 2020, date of current version May 15, 2020.

Digital Object Identifier 10.1109/ACCESS.2020.2990683

A Temporal Sequence Dual-Branch Network for Classifying Hybrid Ultrasound Data of Breast Cancer

ZIQI YANG[1], XUN GONG[1], YING GUO[2], AND WENBIN LIU[3]

[1] School of Information Science and Technology, Southwest Jiaotong University, Chengdu 611756, China
[2] North China University of Science and Technology Affiliated Hospital, Tangshan 063000, China
[3] China Electronics Technologies Cyber Security Co., Ltd., Chengdu 610041, China

Corresponding author: Xun Gong (gongxun@foxmail.com)

This work was supported in part by the National Natural Science Foundation of China under Grant 61876158, and in part by the Sichuan Science and Technology Program under Grant 2019YFS0432.

ABSTRACT In clinical medicine, the contrast-enhanced ultrasound(CEUS) has been a commonly used imaging modality for diagnosis of breast tumor. However, most researchers in computer vision field only focus on B-mode ultrasound image which does not get good results. To improve the accuracy of classification, first, we propose a novel method, *i.e.*, a Temporal Sequence Dual-Branch Network(TSDBN) which, for the first time, can use B-mode ultrasound data and CEUS data simultaneously. Second, we designed a new Gram matrix to model the temporal sequence, and then proposed a Temporal Sequence Regression Mechanism (TSRM), which is a novel method to extract the enhancement features from CEUS video based on the matrix. For B-mode ultrasound branch, we use the traditional ResNeXt network for feature extraction. While CEUS branch uses ResNeXt + R(2 + 1)D network as the backbone network. We propose a TSRM to learning temporal sequence relationship among frames, and design a Shuffle Temporal Sequence Mechanism(STSM) to shuffle temporal sequences, the purpose of which is to further enhance temporal information among frames. Experimental results show that the proposed TSRM could use temporal information effectively and the accuracy of TSDBN is higher than that of state-of-art approaches in breast cancer classification by nearly 4%.

INDEX TERMS Breast cancer classification, temporal sequence, contrast-enhanced ultrasound (CEUS), shuffle mechanism.

I. INTRODUCTION

Breast cancer is the most common cancer of women and the second leading cause of cancer death [1]. Early detection of breast cancer has been shown to significantly improve survival rate of patients [2], [3]. Therefore, correct diagnosis at early stage received widespread attention. Ultrasound has been widely used in the detection of early breast cancer because of its safety, low cost and high versatility [4]. However, its diagnostic accuracy depends on the special skills of the ultrasonic physicians—it says that the diagnosis difference could be larger than 30% among physicians of different levels [5].

In recent years, with the excellent performance of deep learning in image recognition, it has been widely used in ultrasound image classification and has achieved many progresses [6]–[11]. However, most data used by researchers is still B-mode ultrasound images. With the development of medical imaging, contrast-enhanced ultrasound (CEUS) videos can provide more precise pathological information by observing the dynamic enhancement of the lesion area in temporal sequences, and gradually becomes a more effective clinical diagnosis technology than traditional B-mode ultrasound, MRI and CT [12], [13]. Compared with B-mode ultrasound, the related research [14]–[16] show that the CEUS can visualize more sensitive imaging morphology and the flow of microvessels [17], hence, improving the classification accuracy between benign and malignant lesions. Obviously, CEUS contains enhanced information related to lesion that is helpful for breast cancer classification.

Fig. 1 is an example of our hybrid data, in (a) and (b), from left to right, each image is a frame of B-mode ultrasound

The associate editor coordinating the review of this manuscript and approving it for publication was Qichun Zhang.

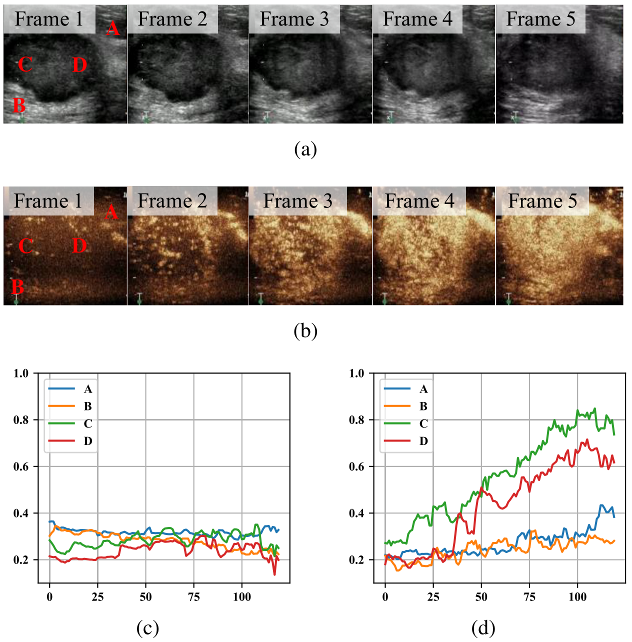

(a)

(b)

(c)

(d)

FIGURE 1. An example of the hybrid ultrasound data used in this work. (a) Different frames of B-mode ultrasound video. (b) Different frames of CEUS video. (c) A curve of brightness values of A, B, C, D in B-mode ultrasound video. (d) A curve of brightness values of A, B, C, D in CEUS video.

video or CEUS video. To measure the discrepancy among frames, according to the characteristics of ultrasound imaging, we use brightness value to quantify different frames. Two points(A, B) in the normal tissue and two points(C, D) in the lesion tissue were selected as measurement points, the results are shown in Fig. 1(c) and (d). It can be seen from the figure that the brightness values of the two tissues only fluctuate slightly in the time dimension of the B-mode ultrasound video. In CEUS video, the brightness value in normal tissue are also only fluctuation punily, but there are largely fluctuations in the lesion tissue. Hence, B-mode ultrasound is a spatial feature which is stable between adjacent frames, while CEUS is a temporal feature as the large variance along timeline. B-mode and CEUS ultrasound represent different perspectives of the lesion area, taking both data as input and designing a unified mechanism to treat them simultaneously will definitely improve the discriminative ability of a classification method for breast tumor.

To this end, we propose a novel method Temporal Sequence Dual-Branch Network(TSDBN), a network for breast cancer classification based on B-mode ultrasound video and CEUS video, the architecture of which is shown in Fig. 2. In the branch of B-mode ultrasound, we use the ResNeXt-18 [18] network to extract the morphological characteristics of breast lesions. In the branch of CEUS, to enhance the temporal feature of CEUS video, we design a Temporal Sequence Regression Mechanism(TSRM) and a Shuffle Temporal Sequence Mechanism(STSM), which make the network pay more attention to the discrepancy among frames along the timeline. First, the TSRM is proposed as a regression mechanism on temporal sequences that indicates the position of different frames in the video. The Gram matrix [19], which is widely used in the field of video generation, is used to express temporal sequences by calculating the distance between different frames in our TSRM block. At the same time, inspired by the method in the fine-grained image classification area [20], in order to enhance the temporal feature of the lesion area, a shuffle temporal sequence mechanism is proposed to disturb adjacent frames. Through STSM, the network will pay more attention to the critical information of CEUS that determine the temporal sequence, which is exactly the benefit that CEUS can provide.

The main contributions of this paper are as follows:

- To the best of our knowledge, for the first time, we proposed a dual-branch framework that uses hybrid data, *i.e.*, B-mode ultrasound video and CEUS video, as input for breast cancer classification. Compared with state-of-art methods, our method has achieved the highest performance.
- A novel temporal feature extraction method, TSRM, of CEUS is proposed, which can extract the dynamic enhanced feature of the lesion area, and uses the shuffle temporal sequence to enhance the temporal feature of video.

This paper is organized by 5 sections: related work is analyzed in Section II. The proposed method is described in Section III. Experiments are conducted and discussed in Section IV. At last, the paper is concluded in Section V.

II. RELATED WORKS

A. BREAST CANCER CLASSIFICATION

Over recent decades, many researchers working on ultrasound have been trying to find a better solution to assist breast tumor diagnosis. Abdel-Nasser *et al.* [21] proposed the use of a super-resolution approach that exploit the complementary information provided by multiple images of the same target. The super-resolution-based approach improves the performance of the evaluated texture methods and thus outperforms the state of art in benign/malignant tumor classification. Alvarenga *et al.* [22] investigated seven morphological parameters in distinguishing malignant and benign breast tumors on ultrasound images and achieved a performance slightly over 83% in distinguishing malignant and benign breast tumors. Mohammed *et al.* [23] presented a fully computerized system (ANN based) to identify and discriminate the benign and malignant breast tumor cases by combining the ultrasound images and the experimental domain information of breast structure. Moreover, Gaussian process classifier is a powerful method for the direct uncertainty quantification of classification application. A breast cancer survivability prediction model that a hybrid of Incremental Learning radial basis function Neural Network, Gaussian Process classifier and AdaBoost can achieve higher prediction accuracy than conventional classifiers. Qi *et al.* [24] proposed a network to diagnose breast ultrasound images using deep convolutional

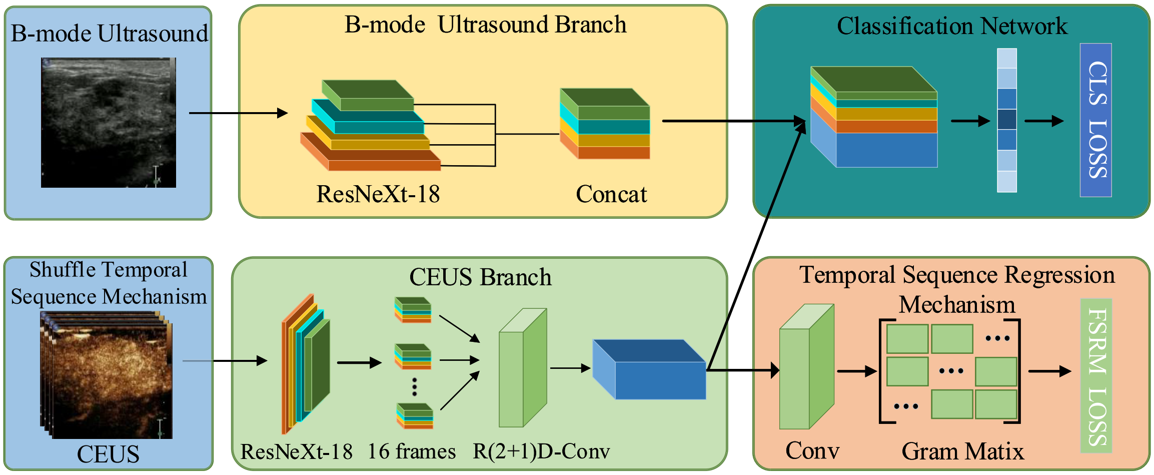

FIGURE 2. The framework of the proposed TSDBN method, including four parts: (1) A Shuffle Temporal Sequence Mechanism: a module for shuffle the input of CEUS video; (2) A dual-branch Network: dual-branch networks extract B-mode ultrasound and CEUS features respectively.; (3) A Classification Network by a fusion of B-mode ultrasound and CEUS features; (4) A Temporal Sequence Regression Mechanism: a loss to make the network pay more attention to the temporal information.

neural networks with multi-scale kernels and skip connections for improve sensitivity and robustness of classification. The network consists of two components to identify malignant tumors and recognize solid nodules in a cascade manner, which improve classification accuracy and sensitivity. Byra *et al.* [25] presented a matching layer for utilize a pre-trained model on the dataset with 3-channel natural images in grayscale ultrasound images. So, the aim of this layer is to rescale pixel intensities of the grayscale ultrasound images and convert those images to red, green, blue (RGB). An experiment results show the usefulness of the approach.

The main shortage of all those methods is that they were working on merely B-mode ultrasound images, lacking context information. Contrast-enhanced ultrasound (CEUS) is the application of ultrasound contrast medium to traditional medical sonography. CEUS has been proved to be more effective in early detection of tumor diagnosis in clinic applications [26]. In the field of ultrasound image analysis, the effectiveness of classification using CEUS data has been studied and proven [27]. Guo *et al.* [28] chosen three typical CEUS images from three phases of CEUS videos, which simulates the clinical diagnosis procedure of radiologists. Then, these images were fed to a multiple kernel learning (MKL) classifier. Pan *et al.* [29] directly used a 3D convolutional neural network (3D-CNN) to extract spatial and temporal features of CEUS. Meng *et al.* [30] presented a method of used B-mode ultrasound and CEUS to classification of liver tumor. Considering the specificity of the two data, the features are extracted from the B-mode ultrasound and CEUS separately, then the features is classified by a multiple empirical kernel learning machine(MEKLM) classifier, which can utilize information of the hybrid data. Although the method have made great achievements in aiding the diagnosis of liver cancer, the drawbacks are obvious. One is that the essential differences between CEUS and B-mode ultrasound have not been further studied. The second is that 3 images only selected from CEUS are not enough to represent the enhancement information of the lesion area. The third is that traditional machine learning methods are used to analyze this hybrid data. Based on this, we revisit many approaches to solve these problems and make further research. To the best of our knowledge, in the field of computer aided ultrasound diagnosis, CEUS video has not been used for automatic breast cancer classification. Therefore, for the first time, we use B-mode ultrasound and CEUS video simultaneously for breast cancer classification.

B. TWO-STREAM METHOD

In the task of video classification based on two kinds of different data, the two-stream method is commonly used. For the first time, Simonyan and Zisserman [31] proposed a two-stream method which uses one stream to learn the spatial context of a single video frame and use another stream to model the motion characteristics from a stacked video optical flow. Then the average fusion is calculated from the *softmax* outputs of two branches. This method provides an instructive direction to combine multimodal data for classification. Further, Feichtenhofer *et al.* [32] analyzed the performance difference of the two-stream networks by using varying fusion strategies, like different ways of integrating spatial features and temporal features. Wang *et al.* [33] proposed a temporal segment network(TSN), which divides a long video into *n* segments, then put *n* segments into two streams respectively, and finally integrates the feature of *n* segments for prediction. This approach aimed to solve the problem that long video is difficult to learn. Lan *et al.* [34] used the weights learned from TSN to evaluate the classification probability of different video segments. Zhou *et al.* [35] put forward a temporal relational network(TRN), which can learn the correlation of objects in the temporal domain between different frames through the network, so that the network is prone to recognize the primary actions. To combine different data for classification, the two-stream-based method can extract the feature of different data independently and fuse them properly. Inspired by the idea of two-stream method, we design a dual-branch network for our hybrid ultrasound data.

C. VIDEO UNDERSTANDING

In the last few years there has been great progress in the field of video understanding. For example, supervised learning and powerful deep learning models can be used to classify a number of possible actions in videos, summarizing the entire clip with a label. Feature representation is the core technique in video understanding. Besides the two-stream method, 3D convolution is another mainstream type of method. Inspired by the Inception-V1 [36], Carreira *et al.* [37] proposed I3D, where 3D convolution kernels of different sizes are used in each inception module and the $1 \times 1 \times 1$ convolution kernels were used for dimensionality reduction. Diba *et al.* [38] put forward the temporal 3D CNN(T3D) to solve the problem of insufficient information mining in the long time domain of 3D convolution. In the network, the author designed the Temporal Transition Layer(TTL) to replace the pooling layer, which has different temporal convolution kernel depths and can capture temporal feature-maps at different temporal depth ranges. Qiu *et al.* [39] proposed a Pseudo-3D Residual Net(P3D ResNet), which uses a 2D space convolution of size $1 \times 3 \times 3$ and 1D time convolution of size $3 \times 1 \times 1$ instead of 3D convolution of size $3 \times 3 \times 3$, which can reduce the number of parameters and achieve better results. Based on the fact that the 2D convolution network has achieved the same accuracy as the 3D network in the field of motion recognition, Tran *et al.* [40] revisited the role of temporal reasoning in action recognition by means of 3D CNN, and proved that factorizing the 3D convolutional filters into separate spatial and temporal components yields significantly gains in accuracy. Finally, a new spatio-temporal convolutional block, R(2 + 1)D is designed, which produces CNN that achieve results superior to the P3D.

Compared with the previous networks are designed from the perspective of convolution along the timeline, some other networks are designed from the perspective of the particularity of video and have also achieved good results. Girdhar *et al.* [41] proposed an Action-VLAD pooling to replace the traditional average pooling and maximum pooling, which can aggregate evidence over the entire video about both the appearance of the scene and the motion of people without requiring every frame to be uniquely assigned to a single action. Considering that an action in most videos are independent of the background, Singh *et al.* [42] proposed a Multi-Stream Network(MSN), which uses a tracking algorithm to extract main object from the background. Along with the original image, the optical flow, the main object are input into a network of four branches. And then the Bi-directional LSTM network is used to extract the temporal feature of the images. As the motion of an object can be regarded as the graph structure of the spatio-temporal domain [43], Wang and Gupta [44] proposed the NGMN, which uses moving objects extracted from video frames to build graph structure, and then uses graph convolution to extract category information from the graph.

D. TEMPORAL SEQUENCE

As for CEUS, the fundamental difference from US is the temporal information provided. Video generation, which is a reversed problem of video analysis, can give us some hints to study temporal information. In order to generate coherent videos, a lot of research has been done on the temporal sequence. Hardy *et al.* [19] introduced the Gram matrix to model the dynamic transformation between consecutive frames, and used the Gram matrix as the motion feature to help network learn the dynamic between video frames. In order to adjust the relationship among frames in a time dimension, a temporal sequence association loss is designed [45], which is to ensure that there will not be too much discrepancy among frames of the video. To guarantee video coherence, the probabilities of start, middle and end points of the video sequence is modeled at the same time, to generate probabilities sequence of action start, action progress and action end [46]. Inspired by video generation, we design a CEUS branch in our network architecture, which uses a regression learning to mining the temporal sequence of CEUS.

III. THE PROPOSED METHOD

Clinically, the combination of B-mode ultrasound and CEUS has become a common technique for breast tumor diagnosis [47]. However, studies on both B-mode image and CEUS video are not well addressed in the field of computer aided ultrasound analysis, as it is hard to find a way to extract useful information from data of different modalities. This paper, a novel method Temporal Sequence Dual-Branch Network(TSDBN) is proposed to classify breast tumor by using both B-mode ultrasound and CEUS video, the architecture of which is shown in Fig. 2. The classical network ResNext-18 is used to extract image feature from B-mode ultrasound directly. For CEUS video, ResNext-18 + R(2 + 1)D [40] is taken as the backbone network. A Temporary Sequence Regression Mechanism(TSRM) and a Shuffle Temporal Sequence Mechanism(STSM) is proposed to promote the extraction capability from CEUS videos. Our network can effectively identify the difference between the original and the destructed CEUS videos, in this way, the temporal enhancement information can be further learned.

A. B-MODE ULTRASOUND AND CEUS DATA

In this paper, inspired by the uses of ultrasound in diagnostics [30], B-mode ultrasound and CEUS video are considered simultaneously to classify breast tumor. They are different expressions of the same lesion area and can help doctors get a better diagnostic image from more perspectives. B-mode ultrasound video riches in shape and texture, see Fig. 1(c), but the pattern and brightness among adjacent frames are stable and rarely has variances. This characteristic of B-mode ultrasound means that there is no additional information in the time dimension. On the other hand, in the CEUS video, Fig. 1(d) has illustrated a clear pattern variances of among different frames in a short period, which means that the pattern in the temporal dimension is evident to provide more pathological information of the lesion area.

B-mode ultrasound image could provide the location, size, shape, internal echo, calcification, and other characteristics of the lesion area. CEUS video could provide dynamic status of the lesion area, including enhancement phase, enhancement intensity, enhancement sequence, enhancement lesion morphology, and other characteristics. Therefore, the B-mode ultrasound video only needs one frame to represent the whole video information. We choose a single frame with the maximum brightness value, denote as S. For CEUS video, in order to reduce the computational complexity and data redundancy, we need to select an appropriate number of frames to represent all the information of the original video as much as possible. Referring to the field of video understanding [35], [38], we use 16 as the number of extracted frames. The formula is as follows,

$$V_{ori} = \left\{ f^j \middle| f^j_{bri} = \frac{[max(f_{bri}) - min(f_{bri})]}{16} \times i + f^1_{bri} \right\} \quad (1)$$

where f^j_{bri} represents the brightness value of j-th frame, we first calculated the maximum($max(f_{bri})$) and minimum ($min(f_{bri})$) value of brightness, then the corresponding frame is selected to from the set of frames(V_{ori}) according to 16 equal division of brightness range. Finally, (V_{ori}, S) as an input to our network. In addition, $i \in \mathbb{N}$ and $0 < i < 16$.

Compared to natural image, lesion region has a rough boundary in B-mode ultrasound image and the contrast is low, which make it difficult to distinguish from the normal tissue. CEUS video is also different from general natural video, which does not contain any movements of an object, only the gradually enhancement of brightness and contrast affected by ultrasound contrast agents injected in the targeted tissues. So, the key is how to extract spatial features from B-mode ultrasound images and temporal features from CEUS video.

B. OVERVIEW OF DUAL-BRANCH NETWORK

As B-mode ultrasound and CEUS video are 2 different modalities, we should design one specific network for each type of data, and then combine them together as an end-to-end hybrid dual-branch network, which is capable of extracting the spatial and temporal features simultaneously.

In the branch of B-mode ultrasound, as shown in Fig.2. ResNeXt-18 [18] is used as the texture and morphological feature extraction. The reason we choose ResNeXt-18 is that, at this stage, we only need to extract some basic and fundamental features, as the basic low-level morphological features are more useful in ultrasound classification. A very deep network will lead to too high-level features, which is not suitable for subsequent network to model temporal information. Moreover, ultrasound dataset is relatively small, a deep network will cause serious overfitting problem. In order to enhance the classification ability of the network, we concatenate the low-level and high-level features into a unified feature.

The shallow convolutional network can diminish the adverse effect of the jitter of CEUS video acquisition and the high noise characteristics of CEUS imaging by a shallow down-sampling. Therefore, in the CEUS branch, we also use ResNeXt-18 as the frame-level feature extractor for the reason. After all feature of 16 frames are obtained, which are then sent to the R(2 + 1)D [40] to extract the temporal feature of this CEUS video. R(2 + 1)D is a common and efficient method to extract temporal features. Compared with the V_{ori}, the frame feature obtained from ResNeXt-18 is more semantic and independent, and is more robustness for further exploiting temporal feature.

Then we concatenate the feature maps(f_{us} and f_{ce}) extracted from S and V_{ori}. After a convolution and a pooling layer, we got the probability vector of the corresponding category. The classification network loss function is defined as follows:

$$\mathcal{L}_{cls} = - \sum_{V, I \in \mathcal{F}} l \cdot \log[C(V_{ori}, S)] \quad (2)$$

where $\mathcal{F}$ is the entire dataset, $C(C(V_{ori}, S))$ represents the classified network output of V_{ori} and S of the sample. $l = 0$ or 1, denotes the category labels, *i.e.*, benign or malignant.

C. TEMPORAL SEQUENCE REGRESSION MECHANISM

When practitioner uses CEUS video to diagnose breast tumor, they mainly observe the enhancement process on images, along the timeline, of the lesion area, such as enhancement phase, enhancement intensity. The enhancement information of lesion areas is contained in different frames, and the different frames have sequence relationship in the time dimension. The sequence relationship is defined as temporal sequence. Therefore, the temporal sequence contains the enhancement information of the lesion area, and the corresponding temporal characteristics of the lesion area can be learned from the temporal sequence. Based on this, the Temporal Sequence Regression Mechanism(TSRM) proposed in CEUS branch to model sequence relationship among frames.

The core problem is to find a tool to express temporal sequences. In MD-GAN [19], Gram Matrix can be used to denote the correlation of two objects. Inspired by this idea, in this paper, the Gram Matrix is used to express the relationship of different frames. Another important key point is how to calculate the temporal correlation among frames. The temporal sequence correlation can be seen as the distance among frames in the time dimension, or discrepancy among frames. From this point of view, according to TGANs-C [45], a temporal sequence label is designed, as shown in Fig. 2(a). The distance between 2 frames is defined as follows:

$$\mathcal{D}(f^i, f^j) = Norm\left(\left\| f^i - f^j \right\|_2 \right), \quad 0 < i, j < 16 \quad (3)$$

Origin Temporal Sequence

$$\begin{array}{c|cccccc|} & 0 & 1 & 2 & 3 & \cdots & 15 \\ \hline 0 & 0 & 0.308 & 0.363 & 0.430 & \cdots & 1 \\ 1 & 0.308 & 0 & 0.327 & 0.396 & \cdots & 0.968 \\ 2 & 0.363 & 0.327 & 0 & 0.380 & \cdots & 0.928 \\ 3 & 0.430 & 0.396 & 0.380 & 0 & \cdots & 0.879 \\ \vdots & \vdots & \vdots & \vdots & \vdots & \ddots & \vdots \\ 15 & 1 & 0.968 & 0.928 & 0.879 & \cdots & 0 \end{array}$$

(a)

Destruction Temporal Sequence

$$\begin{array}{c|cccccc|} & 1 & 0 & 2 & 4 & \cdots & 15 \\ \hline 1 & 0 & 0.308 & 0.327 & 0.395 & \cdots & 0.968 \\ 0 & 0.308 & 0 & 0.363 & 0.430 & \cdots & 1 \\ 2 & 0.327 & 0.363 & 0 & 0.385 & \cdots & 0.928 \\ 4 & 0.395 & 0.430 & 0.385 & 0 & \cdots & 0.859 \\ \vdots & \vdots & \vdots & \vdots & \vdots & \ddots & \vdots \\ 15 & 0.968 & 1 & 0.928 & 0.859 & \cdots & 0 \end{array}$$

(b)

FIGURE 3. An example of Gram matrix label of V_{ori} and V_{des} frame sequence.

where f^i and f^j represent the i-th and j-th frames of a CEUS video, and then the L2-norm is used to measure the temporal sequence distance between 2 frames. The final label format is as follows:

$$M(V_{ori} = \begin{bmatrix} \mathcal{D}(f^1,f^1) & \mathcal{D}(f^2,f^1) & \cdots & \mathcal{D}(f^{16},f^1) \\ \mathcal{D}(f^1,f^2) & \mathcal{D}(f^2,f^2) & \cdots & \mathcal{D}(f^{16},f^2) \\ \vdots & \vdots & \ddots & \vdots \\ \mathcal{D}(f^1,f^{16}) & \mathcal{D}(f^2,f^{16}) & \cdots & \mathcal{D}(f^{16},f^{16}) \end{bmatrix} \quad (4)$$

where $f^1 - f^{16}$ represent 16 frames of the video. It can be seen that $M(V_{ori})$ consists of the distances of all pairs of frames, which can effectively express the enhancement information of the time dimension of video V_{ori}.

TSRM works on the f_{ce} extracted from the CEUS branch to enhance the temporal sequence feature extraction ability. In order to make the output matrix $G(V_{ori})$ of TSRM have the same shape as $M(V_{ori})$, a convolution layer with size of $1 \times 1 \times 1$ is used to reduce the dimensionality of the input feature map, and then an adaptive average pooling layer is used to get the $G(V_{ori})$ of size 16×16. And the TSRM loss is defined as:

$$\mathcal{L}_{TSRM} = \sum_{i=1}^{N}\sum_{j=1}^{N}\left(G(V_{ori})_{(i,j)} - M(V_{ori})_{(i,j)}\right)^2 \quad (5)$$

where $0 < i, j < 16$. This loss calculates the difference between the predicted temporal sequence and the real sequence label. Through solving this regression problem, as we explained ahead, our CEUS branch will gain understandings of CEUS video, and pay more attention to the enhancing procedure of the lesion area in the video.

D. SHUFFLE TEMPORAL SEQUENCE MECHANISM

Shuffle mechanism is used in the field of natural language processing [48] and fine-grained image categorization [20], which local details play a more important role than global structures. The idea of shuffle mechanism could force the network to identify and focus on the discriminative local regions for recognition through destructing global structure and keeping local details. Similarly, if temporal sequence in a video are shuffled, discrepancy among frames that are critical to classification will enhance, and the network will be forced to classify video based on the discrepancy.

Therefore, the shuffle mechanism is used in our temporal sequence of V_{ori}. The principle of this mechanism is to deliberately reorder the 16 frames($f^1 - f^{16}$) extracted from V_{ori}. However, destructing temporal sequence with STSM does not always bring beneficial information, which can lead the temporal sequence to be much confusion. With the use of TSRM, CEUS branch uses the temporal sequence label of V_{des} for regression learning, hence, the network can understand the V_{des} and learn the temporal information. There are two requirements for this mechanism. First, the temporal sequence should not be insufficient destructed, otherwise the V_{des} and the V_{ori} are uniform in temporal sequence information, which will lead to insufficient temporal information for network to learn. Second, the temporal sequence should not be over destructed, otherwise the discrepancy between temporal information of V_{des} and the V_{ori} is too large, in that case the network can not understand the temporal sequence information. Therefore, STSM only shuffles in the neighborhood of one frame, we have:

$$V_{des} = \left\{ f \,\middle|\, \mathit{Shuffle}\left(\left\{f^i, f^{i+1}, \cdots, f^{i+k}\right\}\right), f^i \in V_{ori} \right\} \quad (6)$$

where V_{ori} represents the set of 16 frames selected from the CEUS video, *Shuffle*() is a shuffle function used to shuffle the frames from i to $i+k$ in V_{ori}, and the set of frames after STSM is V_{des}. In addition, $0 < i < 16-k-1$. By elaborately setting the value of k, we make sure that the shuffle is working only in the range of k neighbors of current frame. It can effectively prevent over and insufficient destructed in V_{ori}. By shuffling the V_{ori} properly, the network can not only focus on temporal information of the lesion area, but also solve the problem of data scarcity.

E. TOTAL LOSS

Our network has two outputs, one is classification probability, the other is a temporal sequence relationship matrix. The total loss is computed by:

$$\mathcal{L}_{total} = \alpha\mathcal{L}_{cls} + (1-\alpha)\mathcal{L}_{TSRM} \quad (7)$$

where α is designed to adjust the learning tendency of our network. By adjusting α, the weight of $\mathcal{L}_{cls}$ and $\mathcal{L}_{TSRM}$ in total loss can be changed. Note that the TSRM and STSM block does not need to run in the prediction phase, this can greatly reduce the running time of the network when deploying a model.

IV. EXPERIMENTS

A. DATASET DESCRIPTION

Our hybrid ultrasound dataset consists of 268 samples, 146 are malignant and 122 are benign, each sample contains B-mode ultrasound video, CEUS video and pathological results. All data is collected from the ultrasound department of Sichuan province hospital in China. All samples are reliable and their labels, *i.e.*, benign and malignant, were annotated by physicians. The paper divides the dataset into 10 subsets and uses 10-fold cross-validation to evaluate the performance of the proposed method.

B. IMPLEMENTATION DETAILS

During the training phase, we need to preprocess data to fit the inputs of our network. In the section III we get the input of the network (V_{ori}, S), and use the STSM mechanism to get the V_{des} according to (6). Because of the particularity of the B-mode ultrasound image, conventional data augmentation strategies such as rotation, shift and color jittering are not suitable for this dataset. Only horizontal flip and scale-invariant scaling methods are used for data augmentation in our experiments. For the video frames that do not meet the input shape 256×256 of the network, paddling of 0 is applied. The mini-batch stochastic gradient descent with momentum is used during the optimization. At each iteration, a mini-batch of 8 samples is constructed by sampling a training dataset.

In addition, multiplicative and additive noises in ultrasound images can affect classification results. Therefore, we tried the method based on wavelet transform [51] and the Speckle Reducing Bilateral Filter [52] in ours experiments. However, compared with the original data, we found that did not improve the classification accuracy by using the denoised data. After the analysis, the neural network already has a strong fitting ability, and the 2D convolution has a denoising ability to a certain extent. Therefore, We only use CLAHE [53] to enhance the contrast of ultrasound data in ours experiments.

The learning rate is initially set to 0.001 and then decreased according to a discrete staircase. At the same time, α is a parameter to be set in the network, which can adjust the weight of spatial features and temporal features. The value range is from 0 to 1. In our experiments, we set α to 0.7 to prevent any bias towards the CEUS branch.

In the test phase, the data preprocessing approach is the same as the training phase, but there is no need for STSM analysis. At this stage TSRM need not be computed.

Overfitting is that the production of an analysis that corresponds too closely to a particular set of data, and may therefore fail to fit additional data, which means our model doesn't generalize well from our training data to unseen data. In the paper, we propose a Shuffle Temporal Sequence Mechanism (STSM), which is also a means of data augmentation. The destructed samples will be added to the dataset for training. These methods can guarantee an enough amount of data. At the same time, the R(2 + 1)D that extracts CEUS video features can also avoid the problem of excessive parameter amounts caused by 3D convolution. Overfitting can be prevented by these two approaches.

In order to verify the performance of our proposed method, we use four metrics that are often used in classification tasks, namely accuracy rate(*Acc*), recall rate(*Rec*), precision rate(*Pre*) and $F1_{scroce}(F1)$. $F1$ is a more accurate metric to measure the performance of a binary classifier, which could be expressed as

$$F1 = 2 \times \frac{Rec \times Pre}{Rec + Pre} \tag{8}$$

Due to the particularity in the field of medical classification, the importance of each metric is not the same. *e.g.*, *Rec* weighs over others for tumor detection.

C. PERFORMANCE COMPARISON

To assess the effectiveness of the proposed method, we design different comparison experiments. Since there is no literature on the breast cancer classification with CEUS, we choose the classical and the latest methods of video classification for comparison. All methods are implemented with the author publicly released open-source code, except TRN, LRCN, and NGMN, which code are not released online, we re-implement them in our experiments.

Results listed in Table. 1 has compared our methods with some state-of-art methods. It can be found that *TSDBN_D* has achieved the highest score in classification accuracy, which is 4% higher than other methods. At the same time, it has the highest score in a *Rec*, which can more effectively prevent the missed detection of breast tumor. And for $F1$, *TSDBN_D* also achieves the highest result, compared with the highest 90.2% of other methods, we increased by 3%.

In order to assess the role of CEUS video in different methods, three experiments are carried out: the first experiment only uses B-mode ultrasound image; the second only uses CEUS video; the third uses both data to classify breast tumor. From the results in Table. 1, from the 1st and 2nd row, the best *Acc* is 82.6% using B-mode ultrasound, from 3rd and 4th row, the best result is 83.2% under CEUS video. Combining B-mode ultrasound image and CEUS video, our method can reach to the best *Acc* of 90.2%. This is proved that the temporal information in CEUS video is helpful for breast cancer classification tasks, and the network proposed in the paper can effectively fuse the ultrasound image and CEUS video features together.

In the results of ablated models in Table. 1, we can find that the *Acc* of the model decreases when STSM is added alone. It can be seen that the V_{des} belongs to the wrong sample in the dataset. So the network can not extract the correct temporal information from the V_{des}, which leads to the decline of network accuracy. After adding TSRM, the *Acc* of the model is improved by 2%, which shows that the temporal information extraction ability of our CEUS network can be effectively improved by the regression of learning temporal sequence. When STSM and TSRM are used together, the *Acc* of the network is improved by 4% compared with the original model, and the final *Acc* is up to 90.2%. *Rec* and *Pre* increased by 7.5% and 3.6% respectively, and the $F1$ increased by 4.8%. It can be seen that TSRM can learn the original temporal information of video from the V_{des} by STSM.

The superiority of our method is illustrated more clear in Fig. 4, where (a) and (c) show ROC curves of our method and others. It can be seen that our method has achieved the highest results compared with others. Meanwhile, in the radar charts of (b) and (d), our method outperforms other methods in all four criterion. These results show that the

TABLE 1. The performance comparison of eight methods on the hybrid (ultrasound and CEUS) dataset. The results of four ablated models (TSDBN_A, TSDBN_B, TSDBN_C, TSDBN_D) are shown at the bottom of the table.

Model	TSRM	STSM	Data	Acc	Rec	Pre	$F1$
ResNext-18 [18]			B-mode ultrasound	81.7%	83.4%	79.4%	81.9%
Inception v3 [49]			B-mode ultrasound	82.6%	84.2%	78.7%	82.2%
TRN [35]			CEUS	82.3%	83.5%	81.9%	82.1%
R(2+1)D [40]			CEUS	83.2%	86.4%	83.8%	84.2%
Two-Stream [31]			B-mode ultrasound+CEUS	83.3%	87.4%	82.4%	84.7%
TRN [35]			B-mode ultrasound+CEUS	84.3%	88.6%	86.5%	87.6%
P3D [39]			B-mode ultrasound+CEUS	84.8%	88.9%	88.3%	88.2%
R(2+1)D [40]			B-mode ultrasound+CEUS	86.0%	87.0%	94.4%	90.2%
LRCN [50]			B-mode ultrasound+CEUS	85.7%	83.2%	90.5%	89.8%
MSN [42]			B-mode ultrasound+CEUS	83.6%	81.2%	90.1%	88.5%
Action-VLAD [41]			B-mode ultrasound+CEUS	84.4%	81.9%	92.8%	89.9%
NGMN [44]			B-mode ultrasound+CEUS	81.6%	83.3%	82.8%	85.2%
TSDBN_A	×	×	B-mode ultrasound+CEUS	86.1%	83.9%	91.6%	88.4%
TSDBN_B	×	✓	B-mode ultrasound+CEUS	85.7%	82.6%	90.5%	88.6%
TSDBN_C	✓	×	B-mode ultrasound+CEUS	88.4%	88.9%	94.8%	91.7%
TSDBN_D	✓	✓	B-mode ultrasound+CEUS	**90.2%**	**91.4%**	**95.2%**	**93.2%**

TABLE 2. Comparison of TSDBN_D method and others in terms of parameters, model size, speed, accuracy. The speed is reported on one Nvidia GTX 1080Ti.

Method	Parameters	Model size	Speed	Acc
Two-Stream [31]	17.02M	446MB	9.3 clip/s	83.3%
P3D [39]	9.53M	261MB	**11.8 clip/s**	84.8%
LRCN [50]	**8.63M**	**250MB**	7.6 clip/s	85.7%
Action-VLAD [41]	15.02M	390MB	9.0 clip/s	84.4%
TSDBN_D	9.72M	273MB	11.2 clip/s	**90.2%**

TABLE 3. Comparison of different temporal feature extraction networks.

Network	Acc	Rec	Pre	$F1$
C3D [54]	83.2%	80.4%	80.1%	80.2%
i3D [37]	85.3%	81.2%	82.4%	82.5%
P3D [39]	88.3%	89.5%	89.3%	89.7%
R(2+1)D [40]	**90.2%**	**91.4%**	**95.2%**	**93.2%**
LSTM [55]	83.7%	81.3%	93.3%	84.4%
GRU [56]	84.5%	82.2%	84.3%	86.5%

method proposed in the paper is effective, and our method can learn useful temporal and spatial information from the hybrid data.

To more comprehensively measure our network performance, we compared TSDBN_D method and others in terms of parameters, model size, speed(a video clip contains selected 16 frames from a CEUS video), accuracy, as shown in Table. 2. It can be seen from the table, Two-stream and Action-VLAD have large number of parameters and models size, and leading to a lower speed. The lower speed of Action-VLAD is because VLAD operations requires a lot of calculations. P3D and LRCN have achieved a better quantitative value in terms of parameters and model size and speed. Note the speed of LRCN is the lowest due to the characteristics of RNN. Compared with these methods, TSDBN_D achieves the highest accuracy and good speed with a small amount of parameters and model size. Our model has greater advantages in speed and accuracy. Namely, it's faster and better.

D. MODEL ANALYSIS

The hyper parameters in the method have an impact on the results. These parameters are tunable and can directly affect how well a model can be trained. In this section, we will analyze all hyper parameters adopted in our method one by one.

1) TEMPORAL FEATURE EXTRACTION NETWORK

Temporal feature extraction network is an important part of the CEUS branch. Different network have different feature extraction capabilities. In this paper, several classic temporal feature extraction networks are tested, and the results are shown in Table. 3. In this experiment, we keep the previous experimental settings unchanged, one difference is the temporal backbone network of CEUS branch. It can be seen from the table that R$(2+1)$D obtains the best result in our data. In addition, the methods based on 3D convolution are better than RNN can be found. After analysis, in video, to model temporal information and motion patterns of an object, RNN build temporal connections on the high-level features at the top layer while leaving the correlations in the low-level forms, *e.g.*, edges at the bottom layers, not fully exploited. Compared with RNN, 3D convolution can perform temporal and spatial convolution directly on the frame to obtain more lower-level visual features for model temporal information. Specially, the CEUS video only contains the enhancement process of the lesion area but without motion information, which enhancement modeling is a low/mid-level operate that can be implemented via 3D convolutions. Therefore, 3D-based R$(2+1)$D is more suitable for CEUS video.

2) SHUFFLE GRANULARITY(K)

This is an important hyper parameter in our proposed method, which shows the extent of how we shuffle the temporal

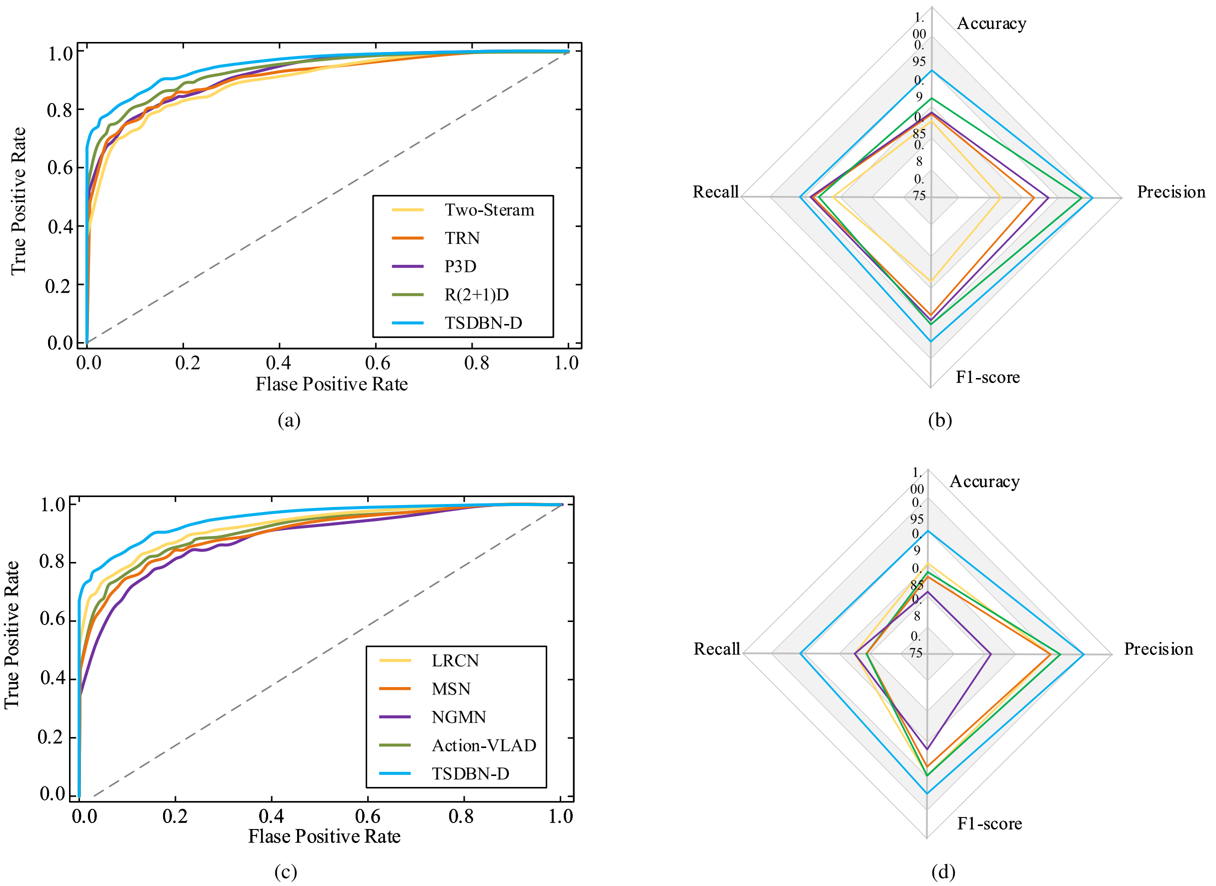

(a) (b) (c) (d)

FIGURE 4. Visualization of different methods from Table. 1 about ROC and four metrics. (a) and (c) are ROC curves of different methods. (b) and (d) are radar charts with four different indexes.

TABLE 4. Performance of TSDBN with different K.

K	Acc	Rec	Pre	$F1$
1	83.3%	87.4%	82.4%	84.7%
2	86.0%	87.0%	94.3%	90.2%
3	**90.2%**	**91.4%**	**95.2%**	**93.2%**
4	87.7%	83.2%	92.4%	83.5%
5	84.2%	80.1%	91.2%	81.2%
7	82.3%	79.0%	89.3%	79.1%
8	79.0%	75.0%	85.0%	76.2%

sequence. From Table. 4, we can find that K has a significant impact on classification accuracy. First, When K value increases, our classification accuracy also increases. Begin from 1, K keeps increasing, the classification accuracy begins to increase as well, and reaches the peak when $K = 3$. Generally speaking, if K is too small, the discrepancies between the disturbed temporal sequence and the original temporal sequence are too small due to the similarity among frames. In that case, the network can not effectively learn the temporal information among different frames. On the contrary, if the K is too large, the discrepancies between the disturbed temporal sequences will be too large, it is hard for the network to converge.

TABLE 5. The classification accuracy of the TSDBN trained with different proportion of V_{ori} and V_{des} in one batch.

Ration	Acc	Rec	Pre	$F1$
1:0	86.2%	83.7%	91.9%	88.4%
1:1	**90.2%**	**91.4%**	**95.2%**	**93.2%**
1:2	87.3%	87.6%	93.5%	88.2%
1:3	86.6%	85.2%	91.2%	87.6%
0:1	84.3%	84.4%	92.4%	84.7%

3) RATIO OF THE V_{des} IN A MINI-BATCH

V_{des} is also a kind of unconventional data augmentation method, and its proportion in a min-batch also affects training results. The paper tests the classification accuracy under different proportions on CEUS videos. The results are shown in Table. 5. When ratio of V_{ori} and V_{des} is set to 1:1 in a batch, the best results are obtained. Too much V_{des} will reduce accuracy, which indicates that too high proportion of V_{des} lead to too much chaos of temporal information. A ratio of 1:0 means STSM is not applied.

4) IMAGE FEATURE EXTRACTION NETWORK

In our method, image feature extraction network is an important part, which directly impacts the performance of the

TABLE 6. Comparisons of different backbone 2D feature extraction network of frame image.

Network	*Acc*	*Rec*	*Pre*	*F*1
VGG-16	85.7%	86.1%	85.8%	86.0%
VGG-19	83.8%	84.2%	84.0%	83.9%
ResNet-18	89.3%	89.4%	93.5%	91.7%
ResNet-50	87.7%	88.0%	91.2%	90.0%
ResNet-101	85.0%	85.5%	87.8%	88.7%
ResNeXt-18(32×4d)	**90.2%**	**91.4%**	**95.2%**	**93.2%**
ResNeXt-50(32×4d)	88.3%	88.9%	91.9%	90.4%
ResNeXt-101(32×4d)	85.7%	85.9%	88.1%	89.2%

following temporal feature extraction. The classic VGG, ResNet and ResNeXt are chosen for comparison in this section, and the results are shown in Table. 6. We find that, interestingly, higher performance can not be obtained by a deeper network, but a shallow network performs even better. Because only build temporal connections on the high-level features at the top layer while leaving the correlations in the low-level forms, e.g., edges at the bottom layers, not fully exploited. Therefore, the low-level features of the frame-level are more useful than high-level features in modeling CEUS videos. Namely, shallow network is more instrumental for our task. in our task. In addition, the low-level features of bottom layers can be transferred to the feature maps of top layers by the residual structure.

V. CONCLUSION

Medical ultrasound analysis has always been a challenging topic in computer vision and pattern recognition. The research in this field has been slow, due to the complexity of the ultrasound images and the lack of large ultrasound data. In this paper, To improve the accuracy of breast cancer classification by ultrasound, for the first time, we combine B-mode ultrasound and CEUS video together, which contain comprehensive and useful pathological information of the lesion area. For this hybrid data, a dual-branch network is proposed to extract spatial features from B-mode ultrasound video and temporal features from CEUS video. In the CEUS branch, we proposed TSRM based on temporal sequence in order to extract the pathological information of CEUS video more efficiently, which helps the network to concentrate on enhancement of the region of lesion in the time dimension. Besides, inspired by the shuffle mechanism, the STSM is designed to enhance temporal information and data augmentation. Finally, the approach suggested in the paper produces the best results in our dataset.

Ultrasound images, like natural images, have uncertainties, which means that the same category may have different appearances, and the same appearance may be different categories. Therefore, to improve the classification ability, one is to improve the amount of train data, the other is to improve the learning ability of the network, including the identification of features and the robustness of the algorithm. In this paper, we mainly explore these two aspects, one is to increase the amount and types of data, the other is to design a network with powerful feature extraction ability.

Data is essential to train a good model for machine learning algorithms or neural networks. To make a better use of data, especially for medical images, it is necessary to design a method from the perspective of physicians. In medicine, it is found that the importance of CEUS video in physicians' pathological judgment is increasing. Therefore, in this work, we use CEUS to assist ultrasound in breast cancer classification, the results are especially promising. Our next work, hence, will still focus on exploiting useful information of CEUS via developing computer vision algorithms.

ACKNOWLEDGMENT

The authors would like to express their gratitude to all those who helped them during the writing of this article. They would like to thank Ms. Zhao and Mr. Irfan for their kind encouragement and useful instructions all through their writing.

REFERENCES

[1] R. L. Siegel, K. D. Miller, and A. Jemal, "Cancer statistics, 2016," *CA, A Cancer, J. Clinicians*, vol. 66, no. 1, pp. 7–30, 2016.

[2] J. Zhang, A. Saha, Z. Zhu, and M. A. Mazurowski, "Breast tumor segmentation in dce-mri using fully convolutional networks with an application in radiogenomics," *Proc. SPIE*, vol. 10575, Feb. 2018, Art. no. 105750U.

[3] M. Yousefi, A. Krzyżak, and C. Y. Suen, "Mass detection in digital breast tomosynthesis data using convolutional neural networks and multiple instance learning," *Comput. Biol. Med.*, vol. 96, pp. 283–293, May 2018.

[4] M. Byra, T. Sznajder, D. Korzinek, H. Piotrzkowska-Wroblewska, K. Dobruch-Sobczak, A. Nowicki, and K. Marasek, "Impact of ultrasound image reconstruction method on breast lesion classification with neural transfer learning," 2018, *arXiv:1804.02119*. [Online]. Available: http://arxiv.org/abs/1804.02119

[5] R. J. Hooley, L. M. Scoutt, and L. E. Philpotts, "Breast ultrasonography: State of the art," *Radiology*, vol. 268, no. 3, pp. 642–659, Sep. 2013.

[6] S. Bhusri, S. Jain, and J. Virmani, "'Classification of breast lesions based on laws' feature extraction techniques," in *Proc. 3rd Int. Conf. Comput. Sustain. Global Develop. (INDIACom)*, Mar. 2016, pp. 1700–1704.

[7] S. Han, H.-K. Kang, J.-Y. Jeong, M.-H. Park, W. Kim, W.-C. Bang, and Y.-K. Seong, "A deep learning framework for supporting the classification of breast lesions in ultrasound images," *Phys. Med. Biol.*, vol. 62, no. 19, pp. 7714–7728, 2017.

[8] S. Y. Shin, S. Lee, I. D. Yun, S. M. Kim, and K. M. Lee, "Joint weakly and semi-supervised deep learning for localization and classification of masses in breast ultrasound images," *IEEE Trans. Med. Imag.*, vol. 38, no. 3, pp. 762–774, Mar. 2019.

[9] A. S. Becker, M. Mueller, E. Stoffel, M. Marcon, S. Ghafoor, and A. Boss, "Classification of breast cancer from ultrasound imaging using a generic deep learning analysis software: A pilot study," *Brit. J. Radiol.*, vol. 31, Dec. 2018, Art. no. 20170576.

[10] M. Byra, M. Galperin, H. Ojeda-Fournier, L. Olson, M. O'Boyle, C. Comstock, and M. P. Andre, "Comparison of deep learning and classical breast mass classification methods in ultrasound," *J. Acoust. Soc. Amer.*, vol. 146, no. 4, p. 2864, Oct. 2019.

[11] V. K. Singh, H. A. Rashwan, M. Abdel-Nasser, M. M. K. Sarker, F. Akram, N. Pandey, S. Romani, and D. Puig, "An efficient solution for breast tumor segmentation and classification in ultrasound images using deep adversarial learning," 2019, *arXiv:1907.00887*. [Online]. Available: http://arxiv.org/abs/1907.00887

[12] V. Cantisani, H. Grazhdani, C. Fioravanti, M. Rosignuolo, F. Calliada, D. Messineo, M. G. Bernieri, A. Redler, C. Catalano, and F. D'Ambrosio, "Liver metastases: Contrast-enhanced ultrasound compared with computed tomography and magnetic resonance," *World J. Gastroenterol.*, vol. 20, no. 29, p. 998, 2014.

[13] X. Wei, Y. Li, S. Zhang, and G. Ming, "Evaluation of thyroid cancer in chinese females with breast cancer by vascular endothelial growth factor (VEGF), microvessel density, and contrast-enhanced ultrasound (CEUS)," *Tumor Biol.*, vol. 35, no. 7, pp. 6521–6529, Jul. 2014.

[14] A. Saracco, B. K. Szabó, P. Aspelin, K. Leifland, E. Tánczos, B. Wilczek, and R. Axelsson, "Contrast-enhanced ultrasound using real-time contrast harmonic imaging in invasive breast cancer: Comparison of enhancement dynamics with three different doses of contrast agent," *Acta Radiologica*, vol. 56, no. 1, pp. 34–41, Jan. 2015.

[15] H.-S. Xia, X. Wang, H. Ding, J.-X. Wen, P.-L. Fan, and W.-P. Wang, "Papillary breast lesions on contrast-enhanced ultrasound: Morphological enhancement patterns and diagnostic strategy," *Eur. Radiol.*, vol. 24, no. 12, pp. 3178–3190, Dec. 2014.

[16] Y. Miyamoto, T. Ito, E. Takada, K. Omoto, T. Hirai, and F. Moriyasu, "Efficacy of sonazoid (perflubutane) for contrast-enhanced ultrasound in the differentiation of focal breast lesions: Phase 3 multicenter clinical trial," *Amer. J. Roentgenol.*, vol. 202, no. 4, pp. W400–W407, 2014.

[17] M. Wubulihasimu, M. Maimaitusun, X.-L. Xu, X.-D. Liu, and B.-M. Luo, "The added value of contrast-enhanced ultrasound to conventional ultrasound in differentiating benign and malignant solid breast lesions: A systematic review and meta-analysis," *Clin. Radiol.*, vol. 73, no. 11, pp. 936–943, Nov. 2018.

[18] S. Xie, R. Girshick, P. Dollár, Z. Tu, and K. He, "Aggregated residual transformations for deep neural networks," 2016, *arXiv:1611.05431*. [Online]. Available: http://arxiv.org/abs/1611.05431

[19] C. Hardy, E. le Merrer, and B. Sericola, "MD-GAN: Multi-discriminator generative adversarial networks for distributed datasets," in *Proc. IEEE Int. Parallel Distrib. Process. Symp. (IPDPS)*, May 2019, pp. 866–877.

[20] Y. Chen, Y. Bai, W. Zhang, and T. Mei, "Destruction and construction learning for fine-grained image recognition," in *Proc. IEEE/CVF Conf. Comput. Vis. Pattern Recognit. (CVPR)*, Jun. 2019, pp. 5157–5166.

[21] M. Abdel-Nasser, J. Melendez, A. Moreno, O. A. Omer, and D. Puig, "Breast tumor classification in ultrasound images using texture analysis and super-resolution methods," *Eng. Appl. Artif. Intell.*, vol. 59, pp. 84–92, Mar. 2017.

[22] A. V. Alvarenga, A. F. C. Infantosi, W. C. A. Pereira, and C. M. Azevedo, "Assessing the performance of morphological parameters in distinguishing breast tumors on ultrasound images," *Med. Eng. Phys.*, vol. 32, no. 1, pp. 49–56, Jan. 2010.

[23] M. A. Mohammed, B. Al-Khateeb, A. N. Rashid, D. A. Ibrahim, M. K. A. Ghani, and S. A. Mostafa, "Neural network and multi-fractal dimension features for breast cancer classification from ultrasound images," *Comput. Electr. Eng.*, vol. 70, pp. 871–882, Aug. 2018.

[24] X. Qi, L. Zhang, Y. Chen, Y. Pi, Y. Chen, Q. Lv, and Z. Yi, "Automated diagnosis of breast ultrasonography images using deep neural networks," *Med. Image Anal.*, vol. 52, pp. 185–198, Feb. 2019.

[25] M. Byra, M. Galperin, H. Ojeda-Fournier, L. Olson, M. O'Boyle, C. Comstock, and M. Andre, "Breast mass classification in sonography with transfer learning using a deep convolutional neural network and color conversion," *Med. Phys.*, vol. 46, no. 2, pp. 746–755, Feb. 2019.

[26] Q. Xiachuan, Z. Xiang, L. Xuebing, and L. Yan, "Predictive value of contrast-enhanced ultrasound for early recurrence of single lesion hepatocellular carcinoma after curative resection," *Ultrason. Imag.*, vol. 41, no. 1, pp. 49–58, Jan. 2019.

[27] L. Qin, H. Yin, H. Zhuang, Y. Luo, P. Liu, and D. C. Liu, "Classification for rectal CEUS images based on combining features by transfer learning," in *Proc. 3rd Int. Symp. Image Comput. Digit. Med. (ISICDM)*, 2019, pp. 187–191.

[28] L. Guo, D. Wang, H. Xu, Y. Qian, C. Wang, X. Zheng, Q. Zhang, and J. Shi, "CEUS-based classification of liver tumors with deep canonical correlation analysis and multi-kernel learning," in *Proc. 39th Annu. Int. Conf. IEEE Eng. Med. Biol. Soc. (EMBC)*, Jul. 2017, pp. 1748–1751.

[29] F. Pan, Q. Huang, and X. Li, "Classification of liver tumors with CEUS based on 3D-CNN," in *Proc. IEEE 4th Int. Conf. Adv. Robot. Mechatronics (ICARM)*, Jul. 2019, pp. 845–849.

[30] F. Meng, J. Shi, B. Gong, Q. Zhang, L. Guo, D. Wang, and H. Xu, "B-mode ultrasound based diagnosis of liver cancer with CEUS images as privileged information," in *Proc. 40th Annu. Int. Conf. IEEE Eng. Med. Biol. Soc. (EMBC)*, Jul. 2018, pp. 3124–3127.

[31] K. Simonyan and A. Zisserman, "Two-stream convolutional networks for action recognition in videos," in *Proc. Adv. Neural Inf. Process. Syst.*, 2014, pp. 568–576.

[32] C. Feichtenhofer, A. Pinz, and A. Zisserman, "Convolutional two-stream network fusion for video action recognition," in *Proc. IEEE Conf. Comput. Vis. Pattern Recognit. (CVPR)*, Jun. 2016, pp. 1933–1941.

[33] L. Wang, Y. Xiong, Z. Wang, Y. Qiao, D. Lin, X. Tang, and L. van Gool, "Temporal segment networks: Towards good practices for deep action recognition," in *Proc. Eur. Conf. Comput. Vis.* Springer, 2016, pp. 20–36.

[34] Z. Lan, Y. Zhu, A. G. Hauptmann, and S. Newsam, "Deep local video feature for action recognition," in *Proc. IEEE Conf. Comput. Vis. Pattern Recognit. Workshops (CVPRW)*, Jul. 2017, pp. 1–7.

[35] B. Zhou, A. Andonian, A. Oliva, and A. Torralba, "Temporal relational reasoning in videos," in *Proc. Eur. Conf. Comput. Vis. (ECCV)*, 2018, pp. 803–818.

[36] C. Szegedy, W. Liu, Y. Jia, P. Sermanet, S. Reed, D. Anguelov, D. Erhan, V. Vanhoucke, and A. Rabinovich, "Going deeper with convolutions," in *Proc. IEEE Conf. Comput. Vis. Pattern Recognit. (CVPR)*, Jun. 2015, pp. 1–9.

[37] J. Carreira and A. Zisserman, "Quo vadis, action recognition? A new model and the kinetics dataset," in *Proc. IEEE Conf. Comput. Vis. Pattern Recognit. (CVPR)*, Jul. 2017, pp. 6299–6308.

[38] A. Diba, M. Fayyaz, V. Sharma, A. H. Karami, M. M. Arzani, R. Yousefzadeh, and L. van Gool, "Temporal 3D ConvNets: New architecture and transfer learning for video classification," 2017, *arXiv:1711.08200*. [Online]. Available: http://arxiv.org/abs/1711.08200

[39] Z. Qiu, T. Yao, and T. Mei, "Learning spatio-temporal representation with pseudo-3D residual networks," in *Proc. IEEE Int. Conf. Comput. Vis. (ICCV)*, Oct. 2017, pp. 5533–5541.

[40] D. Tran, H. Wang, L. Torresani, J. Ray, Y. LeCun, and M. Paluri, "A closer look at spatiotemporal convolutions for action recognition," in *Proc. IEEE/CVF Conf. Comput. Vis. Pattern Recognit.*, Jun. 2018, pp. 6450–6459.

[41] R. Girdhar, D. Ramanan, A. Gupta, J. Sivic, and B. Russell, "Action-VLAD: Learning spatio-temporal aggregation for action classification," in *Proc. IEEE Conf. Comput. Vis. Pattern Recognit. (CVPR)*, Jul. 2017, pp. 971–980.

[42] B. Singh, T. K. Marks, M. Jones, O. Tuzel, and M. Shao, "A multi-stream bi-directional recurrent neural network for fine-grained action detection," in *Proc. IEEE Conf. Comput. Vis. Pattern Recognit. (CVPR)*, Jun. 2016, pp. 1961–1970.

[43] M. Guo, E. Chou, D.-A. Huang, S. Song, S. Yeung, and L. Fei-Fei, "Neural graph matching networks for fewshot 3D action recognition," in *Proc. Eur. Conf. Comput. Vis. (ECCV)*, 2018, pp. 653–669.

[44] X. Wang and A. Gupta, "Videos as space-time region graphs," in *Proc. Eur. Conf. Comput. Vis. (ECCV)*, 2018, pp. 399–417.

[45] Y. Pan, Z. Qiu, T. Yao, H. Li, and T. Mei, "To create what you tell: Generating videos from captions," in *Proc. 25th ACM Int. Conf. Multimedia*, 2017, pp. 1789–1798.

[46] T. Lin, X. Zhao, H. Su, C. Wang, and M. Yang, "BSN: Boundary sensitive network for temporal action proposal generation," 2018, *arXiv:1806.02964*. [Online]. Available: http://arxiv.org/abs/1806.02964

[47] A. Rezo, J. Dahlstrom, B. Shadbolt, K. Rodins, Y. Zhang, and A. J. Davis, "Tumor size and survival in multicentric and multifocal breast cancer," *Breast*, vol. 20, no. 3, pp. 259–263, Jun. 2011.

[48] G. Lample, A. Conneau, L. Denoyer, and M. Ranzato, "Unsupervised machine translation using monolingual corpora only," 2017, *arXiv:1711.00043*. [Online]. Available: http://arxiv.org/abs/1711.00043

[49] C. Szegedy, V. Vanhoucke, S. Ioffe, J. Shlens, and Z. Wojna, "Rethinking the inception architecture for computer vision," 2015, *arXiv:1512.00567*. [Online]. Available: http://arxiv.org/abs/1512.00567

[50] J. Yue-Hei Ng, M. Hausknecht, S. Vijayanarasimhan, O. Vinyals, R. Monga, and G. Toderici, "Beyond short snippets: Deep networks for video classification," in *Proc. IEEE Conf. Comput. Vis. Pattern Recognit. (CVPR)*, Jun. 2015, pp. 4694–4702.

[51] Y. Yue, M. M. Croitoru, A. Bidani, J. B. Zwischenberger, and J. W. Clark, "Nonlinear multiscale wavelet diffusion for speckle suppression and edge enhancement in ultrasound images," *IEEE Trans. Med. Imag.*, vol. 25, no. 3, pp. 297–311, Mar. 2006.

[52] S. Balocco, C. Gatta, O. Pujol, J. Mauri, and P. Radeva, "SRBF: Speckle reducing bilateral filtering," *Ultrasound Med. Biol.*, vol. 36, no. 8, pp. 1353–1363, Aug. 2010.

[53] S. M. Pizer, E. P. Amburn, J. D. Austin, R. Cromartie, A. Geselowitz, T. Greer, B. ter Haar Romeny, J. B. Zimmerman, K. Zuiderveld, "Adaptive histogram equalization and its variations," *Comput. Vis., Graph., Image Process.*, vol. 39, no. 3, pp. 355–368, 1987.

[54] D. Tran, L. Bourdev, R. Fergus, L. Torresani, and M. Paluri, "Learning spatiotemporal features with 3D convolutional networks," in *Proc. IEEE Int. Conf. Comput. Vis. (ICCV)*, Dec. 2015, pp. 4489–4497.

[55] S. Hochreiter and J. Schmidhuber, "Long short-term memory," *Neural Comput.*, vol. 9, no. 8, pp. 1735–1780, 1997.

[56] J. Chung, C. Gulcehre, K. Cho, and Y. Bengio, "Empirical evaluation of gated recurrent neural networks on sequence modeling," 2014, *arXiv:1412.3555*. [Online]. Available: http://arxiv.org/abs/1412.3555

ZIQI YANG received the B.S. degree in computer science from the Weifang University of Science and Technology. He is currently pursuing the M.S. degree with the Department of Computer Science, Southwest Jiaotong University. His research interests include pattern recognition, computer vision, and medical image processing.

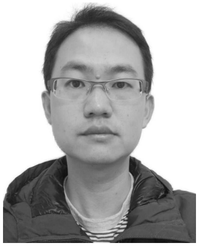

XUN GONG received the B.S. degree in computer science and technology from Beijing Technology and Business University, in 2003, and the Ph.D. degree in computer science and technology from Southwest Jiaotong University (SWJTU), China, in 2008. He was a Visiting Scholar with Alberta University, Canada, in 2015, Louisiana State University, USA, from July 2018 to February 2019. He is currently an Associate Professor with the School of Information Science and Technology, Southwest Jiaotong University. His research interests include pattern recognition, computer vision, medical image processing, and deep learning.

YING GUO received the master's degree from Jinzhou Medical University. She is currently an Ultrasound Doctor with the North China University of Science and Technology Affiliated Hospital. Her research interests include image diagnosis and research of heart disease, thyroid disease, and breast disease.

WENBIN LIU received the B.S. degree in communication engineering from Southwest Jiaotong University, in 2005, and the master's degree in communication and information system from the Beijing University of Posts and Telecommunications, in 2008. He is currently pursuing the Ph.D. degree with the School of Information Science and Technology, Southwest Jiaotong University. He is currently working as a Senior Engineer with China Electronics Technology Cyber Security Company Ltd. His research interests include information security, signal processing, and deep learning.